General model for solar collector fields towards standardization

Report of Bjarne Saxhof's project

Adam Rasmus Jensen and Weiqiang Kong

September 2022

Content

Summary

Being able to accurately model the thermal performance of solar collector fields is essential for introducing new technologies to the market. Characterization of solar collectors is also an important tool in understanding and improving their performance. In this report a generic mathematical model for modeling solar thermal collectors and fields is introduced. The method is applied to three different solar collector fields in Denmark, namely, a flat plate, a parabolic trough, and a Fresnel lens solar thermal collector field. For each collector type, the performance coefficients are derived and discussed. Overall, the applied method was shown to have sufficient accuracy for modeling all the investigated types of solar collectors and is recommended to be used for future standardization and optimization of solar thermal systems.

1. Introduction

Being able to accurately predict the thermal performance of solar thermal technologies is essential to their widespread adoption. For example, without reliable performance estimations, stakeholders cannot make informed decisions of whether to invest in a specific technology and engineers cannot make system optimizations – which is particularly important for emerging technologies. Thus, performance modeling is far from a theoretical exercise, but rather crucial to the adoption of new technologies.

The characterization of solar collectors, which is necessary for making accurate predictions, provides important information about the energy conversion and losses associated with a given system or components. Such information is also crucial in understanding how the technology can be improved and forms the basis for simulation models of solar energy systems.

Accurate performance modeling is particularly important for new solar applications such as solar heating for industrial processes (SHIP), which holds a very large potential due to the large heat demand of industrial processes. Specifically, solar heating can be used to supply heat for industrial applications up to approximately 400 °C. Currently, most of these high-temperature applications utilize fossil fuels as the energy source. As high-temperature solar thermal heating is still a relatively immature technology, there is a strong need to understand the performance and potential of various solutions.

To this end, this report introduces a generic mathematical model for modeling solar thermal collectors and fields. The model is applied to three different solar collector fields in Denmark, namely, a flat plate, a parabolic trough, and a Fresnel lens solar thermal collector field.

2. Mathematical modeling

Several factors influence the performance of solar thermal collectors. The influencing factors can roughly be classified as technological or operational. Technological factors are influenced by the design of the collector, such as how the incident irradiance is converted to heat and the heat loss characteristics. The operational factors include the operating conditions, such as the mean collector temperature and the actual irradiance conditions. Both of these types of factors are necessary to consider when predicting the thermal performance of a solar collector or field.

Over the course of the past 40 years, several mathematical models have been proposed to predict the heat generation of solar collectors. A comprehensive review of test methods and their associated equations are presented in [1]. While many of the available test methods have different strengths, it is important to be able to have a consistent and fair comparison of different collectors. For this reason, standardized procedures have been developed by experts and adopted internationally. One of the most commonly used methodologies is the quasi-dynamic test (QDT) method. The QDT method has also been adopted as one of two ways for collector testing in the international standard ISO 9806 [2].

The QDT method relies on the mathematical formulation of heat generation of a solar collector or field $\dot{Q}$:

$$\dot{Q} = A\begin{bmatrix} \eta_{0,b}K_b(\theta_L,\theta_T)G_b + \eta_{0,b}K_dG_d - a_1(\vartheta_m - \vartheta_a) - a_2(\vartheta_m - \vartheta_a)^2 - a_3u'(\vartheta_m - \vartheta_a) + \\ a_4(E_L - \sigma T_a^4) - a_5(d\vartheta_m/dt) - a_6u'G_{hem} - a_7u'(E_L - \sigma T_a^4) - a_8(\vartheta_m - \vartheta_a)^4 \end{bmatrix} \quad \text{Eq. 1}$$

where the parameters shown in yellow are collector coefficients unique for a specific collector. The parameters shown in blue are measured quantities describing the operating conditions, e.g., mean collector temperature, wind speed, and incident irradiance.

The unknown collector coefficients and incidence angle modifier can be determined from experimental data of the collector operation. The quasi-dynamic method determines the performance coefficients from measurement data using multiple linear regression. The coefficients $\eta_{0,b}$, K_b, K_d, and a_1 through a_8 are constants that describe the heat gain and loss characteristics of a collector or system. The QDT method can also be applied to solar collector fields with minor modifications [3]. In the following sections the QDT method is applied to three existing solar collector fields and its suitability for accurately modeling the solar heat generation is evaluated.

3. Flat plate solar collector field

Denmark has become the front runner in the solar heating plant market with large scale solar collector fields connected to district heating systems. Solar collector fields are composed of solar collectors connected in series and in parallel. An increasing number of large solar collector fields have been built in Denmark in the last years. 125 solar heating plants with a total solar collector area of 1,608,401 m² are in operation by the end of 2021 [4]. Currently, most of the solar collector fields are composed of flat plate solar collectors.

In order to validate the mathematical model and the QDT test method for flat plate solar collector field, one experimental case study was carried out. The experimental verifications focus on flat plate solar collector field operating in Denmark and in situ monitored data were used. The model parameters were derived by implementing Eq.1 and the experimental data, which are compared to the standard lab test results. Then the predicted heat output for the whole collector field were compared to the measured heat output under the measured operating and weather conditions. Figs. 1 and 2 show the hybrid solar heating plant with a 5960 m^2 flat plate collector field and a 4039 m^2 parabolic trough collector field in series in Tårs, Denmark (latitude: 57.39 °N, longitude: 10.11 °E). The plant was put into operation in August 2015.

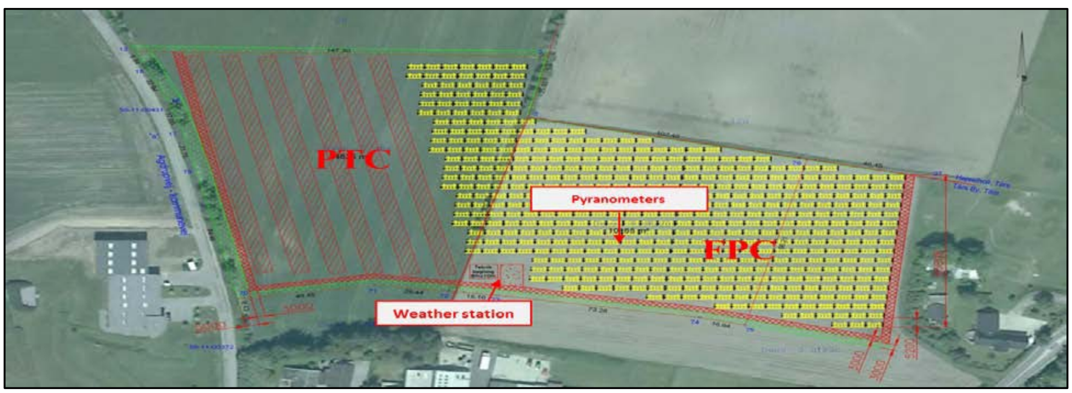

Fig. 1: Layout of solar collector field in Tårs solar heating plant.

Fig. 2: solar collector arrays in Tårs solar heating plant.

Fig. 3 briefly illustrates the basic principle of the solar heating plant. The solar collector fluid for the parabolic trough collectors is water, while that in the flat plate solar collector is a glycol/water mixture (35%/65% in weight). The return water from the district heating network is heated up to 65–75 °C by the heat exchanger connected to the flat plate collector field. Then the preheated water from the flat plate collector field is heated to the required temperature by going through the parabolic trough collector field. The orientation of parabolic trough collector axes was 13.4° towards west from south. The parabolic trough collectors track the sun from east to west when the collectors work during the whole day. There are six rows of parabolic trough collectors and the row distance is 12.6 m. The length of each row of the parabolic trough collector loop is about 125 m. The orientation of the flat plate collectors is due south and the collector row distance is 5.67 m. The tilt of the flat plate collectors is 50°. The flat plate collector field consist of two types of collectors, namely HTHEATboost 35/10 and HTHEATstore 35/10, manufactured by Arcon-Sunmark A/S. Half of the flat plate collector field is made of HTHEATboost 35/10, while the other half is of HTHEATstore 35/10 [5]. Technical data on the flat plate solar collectors and collector field can be found in Table 1.

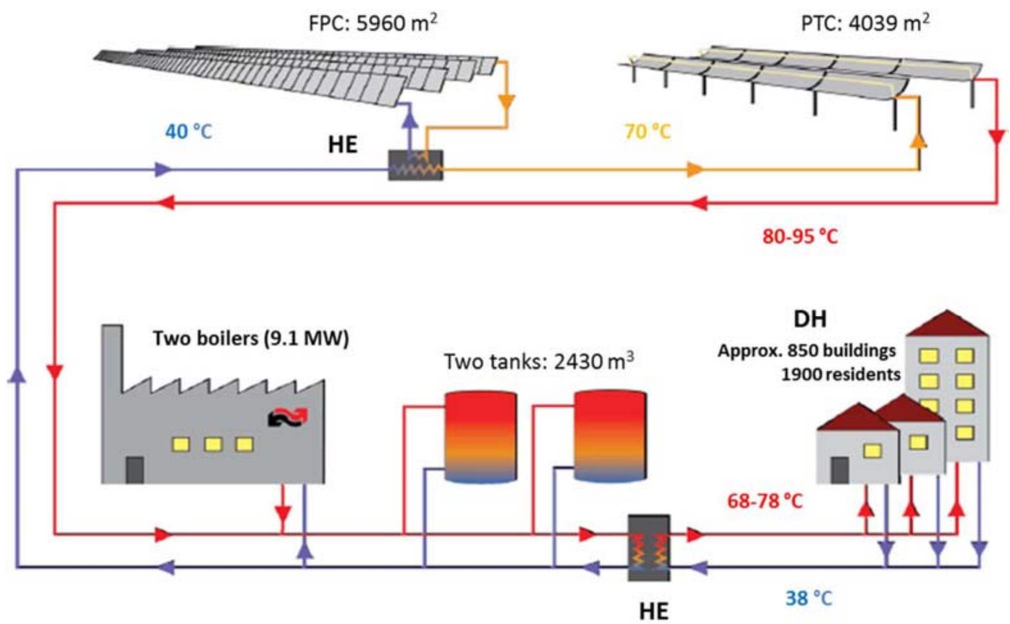

Fig. 3: Schematic diagram of operation principle of Tårs solar heating plant.

Table 1. Information on solar collector and solar collector field.

Flat plate collector		Flat plate collector field	
Aperture area [m^2]	12.60	Aperture area [m^2]	5960
Gross area [m^2]	13.57	Gross area [m^2]	6419
Length [m]	5.96	Row distance [m]	5.67
Width [m]	2.27	Rows [-]	39
Tilt [°]	50	Collector in Row	Typically 6 flat plate collectors without foil and 6 flat plate collectors with foil

Investigations on in situ test of solar collector field will only focus on flat plate solar collector field. The lab test results for the two types of flat plate solar collectors can be seen in Table 2 [5]. The results were taken from standard test sheet based on gross collector area. It can be seen from the table that the flat plate collector with foil has a lower maximum efficiency but also a lower heat loss coefficient than the collector without foil, which is consistent with the expectations.

The in situ model parameters test for the solar collector field was carried out from January 2017 to June 2017. The monitoring system is well equipped with different accurate sensors and the monitoring data are automatically transferred to the computers. Global solar radiation on the horizontal surface and total radiation on the tilted flat plate collectors are measured with Kipp & Zonen SMP11. DNI is measured with a PMO6-CC pyrheliometer with the sun tracking platform Sunscanner SC1. The inlet and outlet temperatures of the collector fields are measured with SIEMENS TS500 temperature sensors, flow rates of both the FPC field and the PTC field are measured with Sitrans FM MAG3100P flow meters - SIEMENS. Measured thermal performance is calculated based on the measured parameters.

The inlet temperature, outlet temperature and flow rate data for the flat plate collector field were taken from the heat exchanger side. Therefore, the whole flat plate solar collector field was monitored during that period. The monitoring time interval is 2 min.

The in-situ test results for the whole solar collector field is also shown in Table 2 as the last column. The field is assumed only to have one collector type. It can be seen from the table that the maximum efficiency of the in situ test result is lower than the two collectors' lab test results, which verified the basic argument of the in situ test method that the maximum efficiency of solar collector fields will be lower than the single collector lab testing. Therefore, the thermal performance prediction by the in situ test method will be more precise than using the parameter data extracted from single collector test report. The heat loss coefficient, diffuse IAM are close to lab test results while the direct IAM and effective capacity have bigger differences compared to the lab test results.

Table 2. Model parameter comparison.

Parameter	**HTHEATboost Lab test**	**HTHEATstore Lab test**	**Flat plate collector field in situ test***
Maximum efficiency η_0 (-)	0.779	0.745	0.706
Direct IAM coeff. b_0 (-)	0.1	0.1	0.24
Diffuse IAM K_d (-)	0.98	0.93	0.78
Heat losses a_1 (W/m^{2}K)	2.41	2.07	2.14
Heat losses a_2 (W/m^{2}K^2)	0.015	0.009	0
Effective capacity a_5 (J/m^{2}K)	6798	7313	3694

The thermal performance prediction was carried out for the whole year of 2016 according to the mathematical model of Eq. 1. The shading effect and incident angle modifier were also calculated based on the deployment of flat plate collector field. The measured useful power output was calculated by the monitored data. The predicted useful power output was calculated by the lab test collector parameters and in situ test collector field parameters separately, together with the measured weather condition and flow rates.
The star * marked in the in situ test results will be discussion at the end of this section.

The measured and predicted useful power output comparison for the whole collector field is shown in single day figures and monthly sums for the whole year 2016. Fig. 4 shows a typical sunny day comparison between measured and predicted power output. The blue curve is the measured power output. The orange curve is the predicted power output using lab test collector parameters while the green is the predicted power output using the in situ test collector field parameters. The orange curve coincides well with the blue curve during the noon period while the green curve fits the blue curve better during the morning and afternoon period. Fig. 5 shows a partly cloudy day comparison and Figs. 6 and 7 show two cloudy day comparisons for the measured and predicted power output. It can be seen from figures that the predicted power output by using lab test results are close to the measured power output mainly in noon periods while the predicted power output using the in situ test collector field parameters are more close to the measured power output mainly in the morning and afternoon period. That is, the lab test results for single solar collector are quite good. But due to the strict QDT test requirements for single collector, the test results can't fit for the whole day period. This could be a hint for further improvement for the QDT single collector test method. The in situ test result seems having bigger difference during noon period compared to the measured result but the result was optimized by minimizing the errors for the whole days, which was verified by the monthly sums in Table 3.

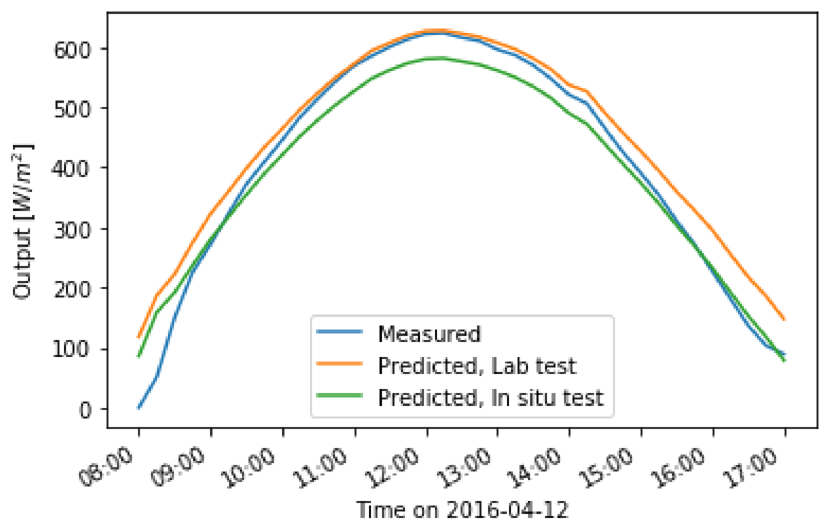

Fig. 4: Measured and predicted power output comparison on 12-04-2016.

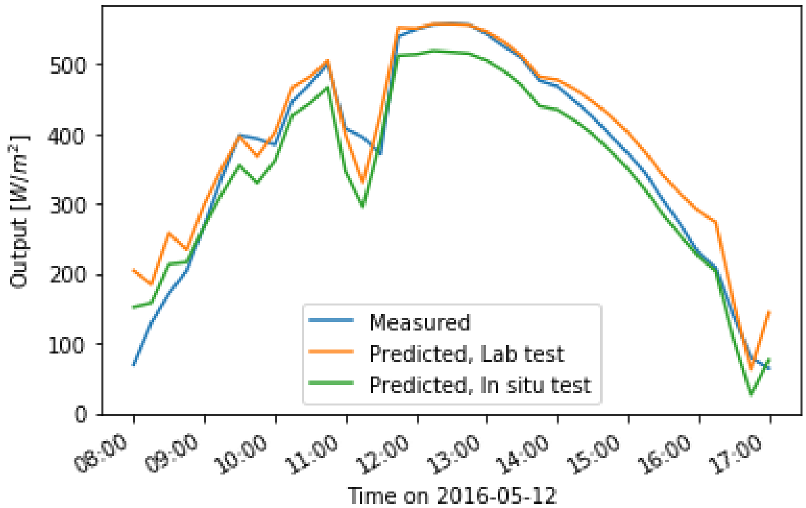

Fig. 5: Measured and predicted power output comparison on 12-05-2016.

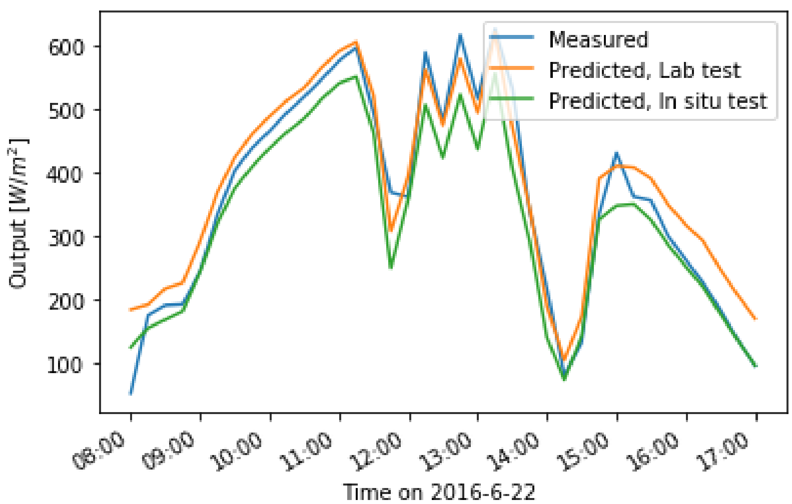

Fig. 6: Measured and predicted power output comparison on 22-06-2016.

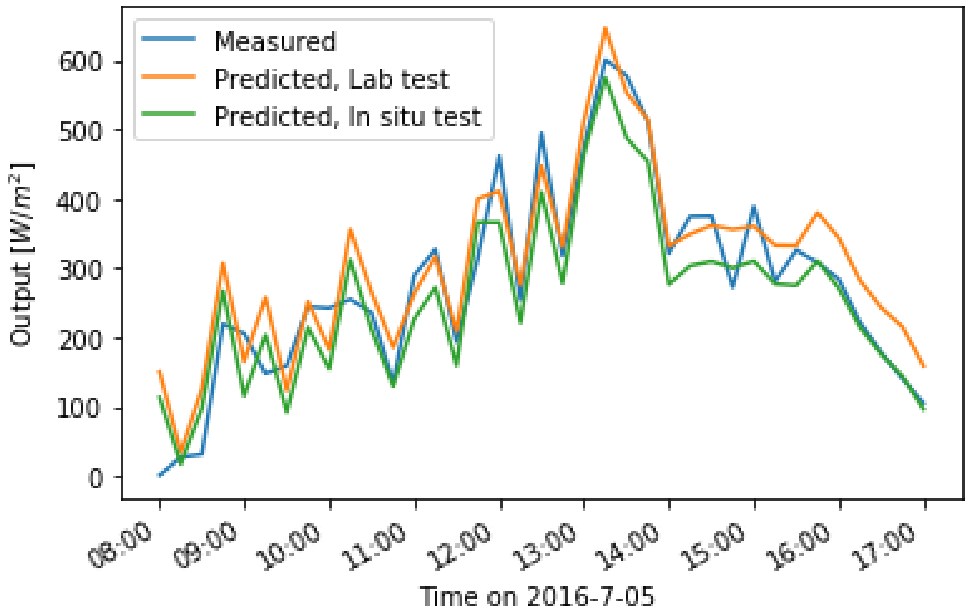

Fig. 7: Measured and predicted power output comparison on 05-07-2016.

Table 3 shows the monthly sums of solar radiation and collector field heat output for the whole year of 2016. The total solar radiation and diffuse solar radiation are listed in column 3 and 4, followed by the measured heat output, modelled heat output using lab test parameters and modelled heat output using in situ test parameters. The last row is the sum of each column.

From the table it can be seen that for the whole year, the total solar radiation on flat plate collector field is 1185 kWh/m^2 while 550 kWh/m^2 was contributed by diffuse solar radiation. The measured heat output of the collector field is 411 kWh/m^2, which is quite close to the modelled heat output by using the in situ test results, 407 kWh/m^2. However, the modelled heat output by using the lab test results is 486 kWh/m^2, which has a larger deviation compared to the measured heat output. The monthly comparison results clearly demonstrate that the in situ test method can predict more precise the heat output for the solar collector field thermal performance compared to the method just using the collector parameters tested from lab.

Table 3. Monthly measured and modelled heat output comparison.

Flat plate collector/ Month	Measured days	Total solar radiation on collector field (kWh/m²)	Diffuse solar radiation (kWh/m²)	Measured heat output (kWh/m²)	Modelled heat output, Lab test (kWh/m²)	Modelled heat output, In situ test (kWh/m²)
01. 2016	31	25	15	2	3	3
02. 2016	28	74	25	21	24	22
03. 2016	31	86	42	28	31	26
04. 2016	30	133	60	48	57	48
05. 2016	31	171	71	67	81	68
06. 2016	30	159	76	60	73	60
07.2016	31	143	85	52	64	51
08.2016	31	142	69	56	65	53
09.2016	30	134	59	56	60	51
10.2016	31	60	22	19	23	20
11.2016	31	33	16	3	5	4
12.2016	30	24	10	1	2	2
Sum	**365**	**1185**	**550**	**411**	**486**	**407**

The developed in situ method uses the modified QDT mathematical model, which is a relative simple model with high accuracy and considers the shading effect in solar collector field. Further, it uses in situ test results for evaluating the thermal performance of solar collector field. By using the in situ test method, the pipe heat losses are considered inherently. The real operating conditions of solar collectors in the field are reflected. In addition, the in situ method uses the weather data from radiation sensors in the field which is an important factor to get accurate results.

Discussion

In Table 2, the in situ test results was marked as start because it was recently found that the measured ambient temperature was not very accurate. The ambient temperature sensor could not be installed correctly, and the values were unusually higher than the typical temperatures in Denmark. Therefore, it is assumed that all the regressed parameters were affected by the problem, especially the heat loss coefficient a1 and the effective thermal capacity a5. Typically, by the proposed method, the large solar collector field including the connecting pipes was assumed as one big collector. So the heat loss coefficient, and the effective thermal capacity should be higher than a single collector. However, the regressed parameters were obtained with lower values. That ‘s why the daily comparison of energy output was not so good by the in situ method. But the monthly total energy output comparison still shows that the in situ test method is better. It can be reasonably estimated that if the ambient temperature were correctly measured, the in situ test method will give a better fit compared to the measured energy output.

4. Parabolic trough solar collector field

Parabolic trough collectors are the most mature type of concentrating solar collector and have been in commercial operation since the 1980s. However, the majority of systems utilizing parabolic troughs have been developed for power generation, and only recently have stakeholders begun focusing on how to utilize this technology for supplying renewable heat to industrial processes and the district heating sector.

As of 2022 there currently exist two systems in Denmark utilizing parabolic trough collectors. The first system is located in Tårs and supplies direct district heating. The parabolic trough collectors in Tårs are utilized in conjunction with flat-plate collectors. The second system is in Brønderslev, where a solar collector field is coupled to a combined heat and power (CHP) biomass plant (see Fig. 8). In Brønderslev, the parabolic trough collectors generate heat up to 320 °C, which can either be used to power an organic Rankine cycle (ORC) turbine which generates electricity, or the solar heat can be fed directly to the district heating network. In the following section, the thermal performance of the Brønderslev solar collector field will be investigated and modeled.

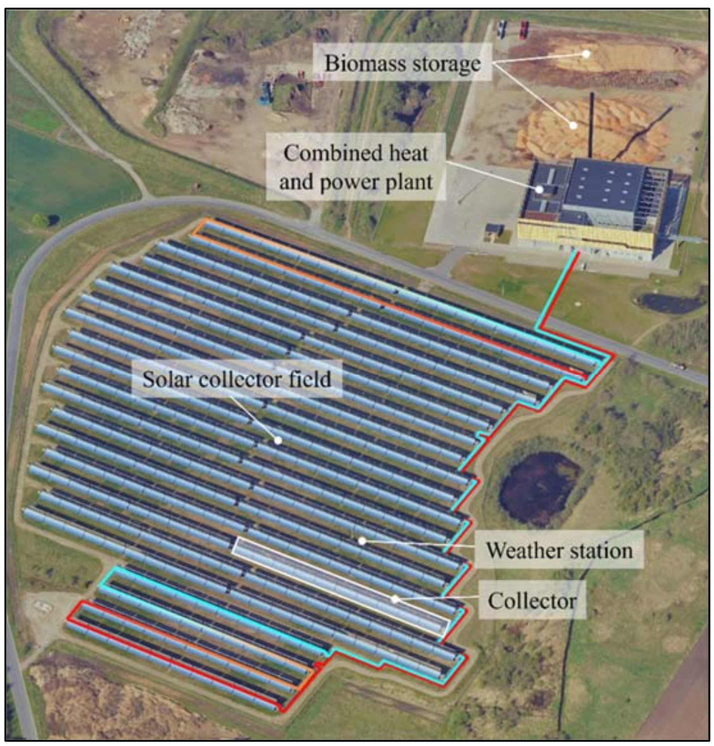

Fig. 8. Aerial view of the Brønderslev hybrid power plant. Pipes to the solar field are marked with blue, and the return pipes are marked red. Image source: the Danish Agency for Data Supply and Efficiency [6].

The Brønderslev solar collector field consists of 40 parabolic trough solar collectors, with a peak thermal output of 16.6 MW. The solar collector field covers an area of 9 hectares with a total mirror (aperture) area of 26,930 m^2. Construction of the parabolic trough solar collector field began in 2016, and operation started in January 2017.

Each of the solar collectors has a width of 5.77 m and a length of 120 m. The parabolic trough collectors were manufactured by the Danish company Aalborg CSP and are the company's fourth-generation parabolic trough collectors (AAL-TroughTM 4.0). The parabolic troughs are single-axis tracking, with a tracking axis 30° east of north.

To quantify the thermal performance of the collector field, it is characterized using the quasi-dynamic test method to obtain the performance coefficients (shown in blue in Eq. 1). Measurement data of the actual solar field operation from 5 May to 31 October 2020 was used to derive the coefficients.

It should be noted that [7] recommends the incidence angle modifier for parabolic trough collectors is recommended to be modeled using the methodology proposed in [8]:

$$K_b(\theta_L) = 1 - \frac{(b_1 \cdot \theta_L + b_2 \cdot \theta_L^2)}{\cos(\theta_L)} \quad \text{Eq. 2}$$

The performance coefficients identified for the Brønderslev solar field using the QDT method are listed in Table 4. In addition to the value of the coefficients, the table also presents the standard deviation and t-score for each coefficient. Note, the QDT method specifies that any coefficient with a t-score less than three should be omitted, as it is not sufficiently statistically significant. This was the case for a2, a8, and b2, hence these coefficients are not included in the table.

Table 4. Performance coefficients of the Brønderslev parabolic trough collector field.

Parameter	Value	Std. dev.	T-score	Unit
$\eta_{0,b}$	72.7%	0.6%	113	-
a_1	0.271	0.032	8.5	W/(m^2 K)
a_5	6741	146	46	J/(m^2 K)
b_1	2.6×10^{-3}	0.1×10^{-3}	25	(°)$^{-1}$

It is important to note that the coefficients in Table 4 correspond to the entire collector field, including approximately 1200 m of piping that connects the solar collector loops to the power plant. Specifically, this means that the heat loss coefficient (a1) accounts for the heat losses from the PTCs and the pipes, and the heat capacity (a5) includes the additional thermal capacity of the fluid in the pipes and the piping itself.

Furthermore, to test the validity of the derived coefficients, the coefficients were used in a simple simulation model to predict the solar collector field performance during validation period. The modeled and measured data for five days of the validation period are shown in Fig. 9. The top subplot shows a comparison of the measured and modeled heat generation. Based on the generation profile, it can be observed that the first day was relatively clouded, the second day had drifting clouds, and the remaining days were mainly clear sky. For the entire period shown, the measured and modeled heat generation matched well. This confirms the validity of the performance coefficients determined previously and demonstrates that characterization results and method is suitable for accurately modeling the collector field output. The remaining subplots are further discussed in [6].

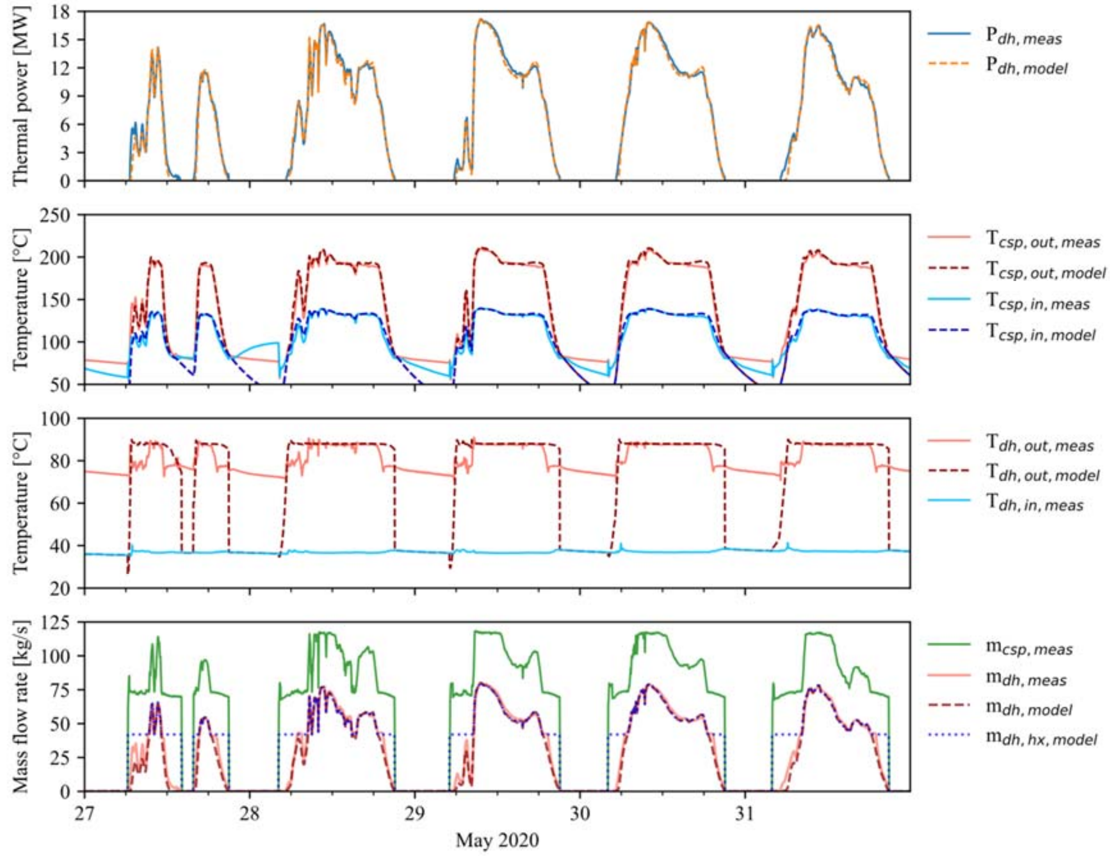

Fig. 9. Comparison of measured and modeled values for five days in 2020 [6].

The measured and modeled heat generation is also compared in Fig.10 in terms of hourly average values. The scatter plot shows that there is only a small variation between the measured and predicted heat generation, indicating that the simulation model is able to accurately capture the system performance. The root-mean-square error (RMSE) of the predicted heat generation is 0.2 MW. The model exhibited a slight negative bias of 2%, meaning that the model has a tendency to underestimate heat generation in the long term. Overall, the model performance can be considered satisfactory, and the validated model and parameters can be used for future optimization studies, aiding in achieving optimal plant design.

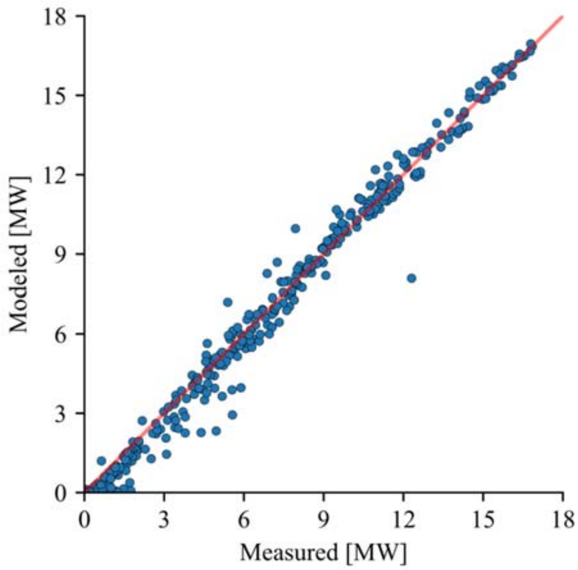

Fig.10. Comparison of modeled and measured hourly average heat generation from the Brønderslev parabolic trough solar collector field [6].

In this section, the Brønderslev solar collector field was characterized using the quasi-dynamic test method. The peak efficiency of the solar collector field was found to be 72.7%. This value is somewhat lower than previous studies of the same system, which suggests that the location has mild soiling conditions. Furthermore, the heat loss and thermal capacity coefficients were found to be more than twice as high compared to a single collector. The reason for this is that the determine coefficients were for the entire field, as thus also include the effects of the field piping.

5. Fresnel lens solar collector field

Fresnel lens solar collectors are a relative new technology, and thus not much has been known about the potetnail performance of such collectors. The main innovation in the technology is being led by the Danish company, Heliac, which has developed a Fresnel lens solar collector for district heating and industrial applications. The Heliac collector is a point-focusing solar collector, which concentrates the solar radiation using eight Fresnel lenses. The Fresnel lens is made of a polymer film and is applied to the backside of a float glass. Due to a novel roll-to-roll manufacturing process, the Fresnel lens collectors be made at a very low cost.

The solar collector field in Lendemarke consists of 144 two-axis tracking Fresnel lens solar collectors. The concentrating solar collector were manufactured by the Danish company Heliac. The solar collector field spans almost one hectare and is located near the town of Lendemarke, Denmark (latitude: 54.979 °N, longitude: 12.267 °E). A photo of the collector field during operation is shown in Fig. 11. The heat generated from the solar collectors is supplied to the accumulation tank of the local district heating plant.

Fig.11. Photo of the Fresnel lens solar collector field, Lendemarke, Denmark.

To assess the performance of the Lendemarke Fresnel solar collector field, the QDT method was applied in order to obtain the performance coefficients. Measurements from 10 days between March 15th and April 10th, 2021, were used to derived the performance coefficients. This period was chosen as the plant operated continuously during this period and DNI measurements were available. The performance coefficients for the Lendemarke Fresnel lens collector field are listed in Table 5.

Table 5. Performance coefficients of the Lendemarke collector field [9].

Parameter	Field coefficients	Std. error (field coef.)	Collector coefficients [10]	Unit
$\eta_{0,b}$	0.535	0.01	0.602	-
K_d	-	-	0.02	-
a_1	1.62	0.16	0.23	W/(m^2 K)
a_3	-	-	0.178	J/(m^3 K)
a_5	11 500	1 000	3 360	J/(m^2 K)

The QDT characterization of the Lendemarke solar collector field found a peak efficiency of 53.5%, a first order heat loss coefficient of 1.62 W/(m^2 K). The effective thermal capacity of the field was found to be 11.5 kJ/(m^2 K). The performance coefficients and their standard errors are given in Table 5.

The performance coefficients derived for a single clean Heliac collector in [10] are also presented in Table 5. These coefficients are for a single brand-new collector and thus do not account for connecting pipes and soiling. Therefore, the peak efficiency is expected to be lower under actual operation due soiling. Similarly, the heat losses and thermal capacity will be higher for the collector field due to additional piping. The peak efficiency of the Lendemarke solar field found to be 11% lower than the values provided in the single collector test report. This reduction in the peak efficiency is primarily caused by soiling, as the collectors were exposed to outdoor conditions for more than one year without any cleaning.

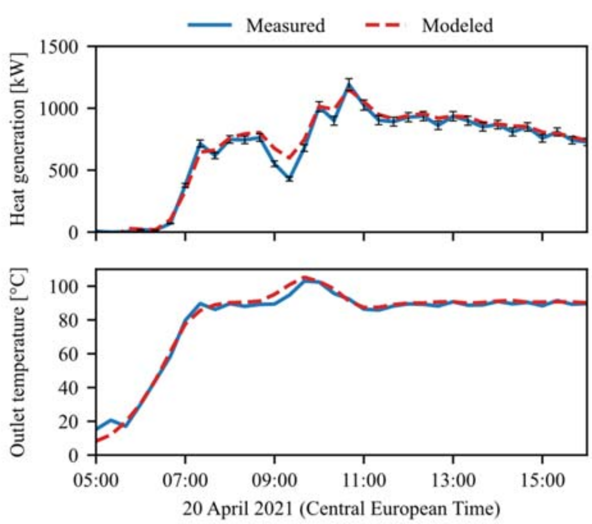

Fig.12. Comparison of the measured and modeled heat generation for the Lendemarke solar collector field [9].

To validate the performance coefficients, the operation of the solar field was simulated for the validation period and compared to measurements of the actual operation. A comparison of the heat generation and collector field outlet temperature is shown in Fig. 12 for one day. The figure shows that the simulated values match well the measurements, thus the performance coefficients were able to accurately model the thermal performance.

A comparison of the modeled and measured heat generation for the entire validation period is shown in Figure 13. The scatter plot shows the average heat generation for one hour. Overall, there is a minor deviation between the modeled and predicted values, with a high prediction accuracy at the low and high end of the generation spectrum. Notably, the simulation model has a small tendency to overestimate the heat generation in the range of 600-900 kW and with an overall positive bias of 1.8 %. It can thus be concluded that the modeling methodology is suitable for making accurate predictions of the performance of large scale solar heating systems.

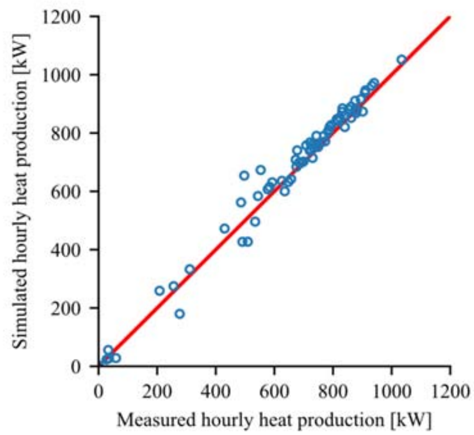

Fig.13. Comparison of simulated and modeled heat production from the Lendemark solar collector field [9].

Nomenclature

A	Collector area
a_1	Heat loss coefficient
a_2	Temperature dependence of heat loss coefficient
a_3	Wind speed dependence of heat loss coefficient
a_4	Sky temperature dependence of heat loss coefficient
a_5	Effective thermal capacity
a_6	Wind speed dependence of zero loss efficiency
a_7	Wind speed dependence of IR radiation exchange
a_8	Radiation losses
b_1	First order IAM coefficient
b_2	Second order IAM coefficient
σ	Stefan-Boltzmann constant
E_L	Longwave irradiance
G_{hem}	Hemispherical solar irradiance
G_b	Beam irradiance
G_d	Diffuse irradiance
K_b	IAM for direct solar irradiance
K_d	IAM for diffuse solar radiation
$\dot{Q}$	Useful heat
T_a	Sky temperature
u	Wind speed
u'	Reduced air speed (u – 3 m/s)
$\eta_{0,b}$	Peak collector efficiency based on G_b
ϑ_m	Mean temperature of the heat transfer fluid
ϑ_a	Ambient air temperature
θ_L	Longitudinal incidence angle
θ_T	Transversal incidence angle

Reference

[1] P. Obstawski, T. Bakoń, and D. Czekalski, “Comparison of Solar Collector Testing Methods—Theory and Practice,” *Processes*, vol. 8, no. 11, p. 1340, Oct. 2020.

[2] ISO 9806, “Solar energy - Solar thermal collectors - Test methods,” 2017.

[3] F. Sallaberry, Z. Tian, B. Perers, S. Furbo, A. Zourellis, and J. H. Rothmann, “On-site parabolic-trough collector characterization in solar district heating plant under quasi-dynamic conditions,” *AIP Conf. Proc.*, vol. 2126, 2019.

[4] Werner Weiss, Monika Spörk-Dür. Solar Heat Worldwide. Edition 2022. IEA SHC.

[5] Z. Tian, B. Perers, S. Furbo, and J. Fan, “Annual measured and simulated thermal performance analysis of a hybrid solar district heating plant with fl at plate collectors and parabolic trough collectors in series,” *Appl. Energy*, vol. 205, no. July, pp. 417–427, 2017.

[6] A. Jensen and I. Sifnaios, “Modeling, Validation, and Analysis of a Concentrating Solar Collector Field Integrated with a District Heating Network,” *Solar*, vol. 2, no. 2, pp. 234–250, May 2022.

[7] IEC, “IEC 62862 Part 3-2 : Systems and components – General requirements and test methods for large-size parabolic-trough collectors,” 2018.

[8] L. Valenzuela, R. López-Martín, and E. Zarza, “Optical and thermal performance of large-size parabolic-trough solar collectors from outdoor experiments: A test method and a case study,” *Energy*, vol. 70, pp. 456–464, 2014.

[9] A. R. Jensen, I. Sifnaios, G. P. Caringal, S. Furbo, and J. Dragsted, “Thermal performance assessment of the world’s first solar thermal Fresnel lens collector field,” *Sol. Energy*, no. January, Mar. 2022.

[10] A. R. Jensen, “Test of Heliac 3rd Gen. Solar Collector,” in *DTU Byg report no. R-443*, 2020.